# ENCORE: An Extended Contractor Renormalization algorithm

A. Fabricio Albuquerque,[1,2] Helmut G. Katzgraber,[1,3] and Matthias Troyer[1]

[1]*Theoretische Physik, ETH Zurich, 8093 Zurich, Switzerland*
[2]*School of Physics, The University of New South Wales, Sydney, NSW 2052, Australia*
[3]*Department of Physics, Texas A&M University, College Station, Texas 77843-4242, USA*

(Dated: September 18, 2018)

Contractor renormalization (CORE) is a real-space renormalization-group method to derive effective Hamiltonians for microscopic models. The original CORE method is based on a real-space decomposition of the lattice into small blocks and the effective degrees of freedom on the lattice are tensor products of those on the small blocks. We present an extension of the CORE method that overcomes this restriction. Our generalization allows the application of CORE to derive arbitrary effective models whose Hilbert space is not just a tensor product of local degrees of freedom. The method is especially well suited to search for microscopic models to emulate low-energy exotic models and can guide the design of quantum devices.

PACS numbers: 87.55.kd,03.67.Ac,02.70.-c,03.67.Pp

## I. INTRODUCTION

Identifying the emergent low-energy degrees of freedom in a strongly-correlated system is a highly nontrivial problem requiring considerable physical intuition and a careful analysis of available experimental data [1]. The contractor renormalization (CORE) method introduced by Morningstar and Weinstein [2, 3] is a tool to systematically perform this task: by suitably selecting low-energy local degrees of freedom and applying a real-space renormalization procedure, one can in principle obtain an effective Hamiltonian which is simpler than the original one and therefore (ideally) more amenable to subsequent analytical or numerical treatment. For recent applications of CORE see, for example, Refs. 4, 5, 6, 7, 8, 9.

The idea behind CORE is to divide the lattice on which the model is defined into blocks and to retain only a small number of suitably chosen low-lying block eigenstates. The low-energy eigenstates of the full Hamiltonian defined on a cluster formed by two or more blocks are then projected onto the restricted basis formed by tensor products of the retained block states. By requiring that the low-energy spectrum of the full problem is exactly reproduced, an effective Hamiltonian is obtained. The mapping onto a coarser-grained lattice with redefined degrees of freedom is done at the expense of having longer-range effective interactions. A successful application of the method relies on a fast decay of the effective interactions, which in turn depends on the correct choice of the effective degrees of freedom and on the particular way the lattice is divided into blocks, as well as on how the retained block eigenstates are chosen. Because physical intuition and a good idea of the relevant local degrees of freedom are needed to obtain physically sound results, we believe that this is the main reason why CORE has not found a more widespread use.

The "inverse" problem of using CORE to find microscopic models that map well onto a desired effective low-energy Hamiltonian does not suffer from the aforementioned problems: because the emergent degrees of freedom are known *a priori* and their adequacy in describing the low-energy physics of the device is *enforced* by design, the aforementioned limitations of CORE can be used to our advantage. Whenever the effective Hamiltonian includes sizable long-range interactions and/or states with a vanishing projection on the restricted basis are present in the low-energy spectrum, one can conclude that the considered microscopic model is not well approximated by the proposed low-energy effective model. Given current interest in the emulation of exotic phases via physical models (e.g., by using Josephson junctions or cold atomic/molecular gases), we expect this approach to be useful when designing manipulable *quantum tool boxes*. Finally, we note that the step of dividing the lattice into blocks is no longer required or even desirable within this context and we thus extend the method to models built from geometrically-constrained degrees of freedom, such as quantum dimer models [10, 11], where the emergent degrees of freedom cannot be described in terms of tensor products of local states. Below we introduce an extension of the CORE method applicable to arbitrary basis states of the effective model and illustrate the application of the method with an array of quantum Josephson junctions [12] used to implement a topologically protected qubit [13].

## II. EXTENDED CORE METHOD

We first review the standard CORE algorithm [2, 3, 14, 15] and then contrast it to the extended CORE (dubbed ENCORE) method proposed here.

### A. Standard CORE algorithm

Given a Hamiltonian $\mathcal{H}$ defined on a lattice $\mathcal{L}$, the standard CORE algorithm can be described as follows:

1. Divide the lattice $\mathcal{L}$ into disconnected small blocks $\mathcal{B}$ and diagonalize the Hamiltonian $\mathcal{H}$ within a single block, keeping $M$ low-lying eigenstates $\{|\phi_m\rangle\}_1^M$. The subspace spanned by tensor products of these block eigenstates on a cluster $\mathcal{C}$—formed by joining a number of elementary blocks—defines the reduced Hilbert space within which the effective model is derived.

2. Diagonalize $\mathcal{H}$ on a cluster $\mathcal{C}$ consisting of $N$ connected blocks retaining the $\mathcal{M} = M^N$ lowest eigenstates $\{|n\rangle\}_1^{\mathcal{M}}$ with energies $\epsilon_n$ and project them onto the basis formed by the tensor products of the block states, $\{|\phi_{m_1}, ..., \phi_{m_N}\rangle\}_1^{\mathcal{M}}$, forming the projected states $\{|\psi_n\rangle\}_1^{\mathcal{M}}$.

3. Orthonormalize the obtained projected states $\{|\psi_n\rangle\}_1^{\mathcal{M}}$ using a Gramm-Schmidt procedure

$$|\tilde{\psi}_n\rangle = \frac{1}{Z_n}\left(|\psi_n\rangle - \sum_{m<n} |\tilde{\psi}_m\rangle\langle\tilde{\psi}_m|\psi_n\rangle\right), \tag{1}$$

where $Z_n$ stands for the normalization of the orthogonalized state.

4. The range-$N$ renormalized Hamiltonian is then

$$\mathcal{H}_N^{\text{ren}} = \sum_n^{\mathcal{M}} \epsilon_n |\tilde{\psi}_n\rangle\langle\tilde{\psi}_n|. \tag{2}$$

By construction, this Hamiltonian has the same low-energy spectrum as the original one.

5. Writing Eq. (2) in terms of the tensor product states $\{|\phi_{m_1}, ..., \phi_{m_N}\rangle\}_1^{\mathcal{M}}$, we obtain the range-$N$ effective interactions between the blocks forming the cluster after subtracting the previously calculated shorter-range interactions

$$h_{i_1 \ldots i_N} = \mathcal{H}_N^{\text{ren}} - \sum_{N'=1}^{N-1} \sum_{\langle i_1, \ldots, i_{N'}\rangle} h_{i_1 \ldots i_{N'}}, \tag{3}$$

where $\langle i_1, ..., i_{N'}\rangle$ denotes the set of *all connected* range-$N'$ subclusters. The effective range-$N$ Hamiltonian can then be written as

$$\mathcal{H}_N^{\text{eff}} = \sum_i h_i + \sum_{\langle i,j\rangle} h_{ij} + \sum_{\langle i,j,k\rangle} h_{ijk} + \ldots, \tag{4}$$

where $h_i$ is the block self-energy, $h_{ij}$ the interaction between nearest-neighbor blocks, $h_{ijk}$ a three-block coupling, etc. up to range-$N$ interactions.

The successful application of the above procedure relies on a fast decay of the long-ranged effective interactions appearing in Eq. (4) and therefore one chooses the restricted set of degrees of freedom by specifying the elementary blocks $\mathcal{B}$ and the retained block states $\{|\phi_m\rangle\}_1^M$.

### B. ENCORE algorithm

It is possible to extend the ideas presented in Sec. II to constrained effective models—e.g., quantum dimer models, loop models, and string nets—for which the relevant degrees of freedom are no longer formed by tensor products of block states but, instead, by the set of configurations on a given cluster satisfying the constraints of the Hamiltonian to be emulated. We thus present an extended algorithm using alternative ways of selecting the restricted degrees of freedom.

1. Choose a finite-size cluster $\mathcal{C}$ and build a basis $\{|\phi_m\rangle\}_1^M$ for the Hilbert space of the effective model. In the standard CORE method this effective basis is a tensor product of the relevant states on the blocks, whereas here it is comprised by all constrained configurations on $\mathcal{C}$. For example, for a quantum dimer model we generate all $M$ possible dimer coverings on the cluster $\mathcal{C}$.

2. Diagonalize $\mathcal{H}$ on the cluster $\mathcal{C}$, calculating the $M$ lowest eigenstates $\{|n\rangle\}_1^M$ with energies $\epsilon_n$ and project them onto the restricted basis $\{|\phi_m\rangle\}_1^M$, forming the projected states $\{|\psi_m\rangle\}_1^M$ [16].

3. Orthonormalize by means of a Gramm-Schmidt procedure as in Eq. (1).

4. The Hamiltonian within the restricted space is then given by Eq. (2).

5. Writing this Hamiltonian in the restricted basis $\{|\phi_m\rangle\}_1^M$ we obtain the effective model

$$\mathcal{H}^{\text{eff}} = \sum_{m,m',n}^{M} \epsilon_n |\phi_m\rangle\langle\phi_m|\tilde{\psi}_n\rangle\langle\tilde{\psi}_n|\phi_{m'}\rangle\langle\phi_{m'}|. \tag{5}$$

It is again possible to perform a cluster expansion within ENCORE by using Eqs. (3) and (4).

Note that the above discussion is for an orthonormal restricted basis $\{|\phi_m\rangle\}_1^M$, such as in the example discussed in Sec. III. Small changes in the procedure are required if this is not the case [10].

## III. APPLICATION: EMULATION OF THE QUANTUM DIMER MODEL

### A. Array of quantum Josephson junctions

We apply the algorithm described in Sec. II B to extract the dimer flip amplitude $t$ for a Josephson-junction array introduced by Ioffe *et al.* [12] to emulate a quantum dimer model (QDM) [10] on a triangular lattice. This model—first investigated by Moessner and Sondhi [11]—has the desired properties needed to implement a topologically protected qubit and is given by $\mathcal{H} = \mathcal{H}_{\square} + \mathcal{H}_{\square} + \mathcal{H}_{\square}$ with

$$\begin{aligned}\mathcal{H}_{\square} = &-t \sum_{\square} \left[|\square\rangle\langle\square| + |\square\rangle\langle\square|\right] \\ &+v \sum_{\square} \left[|\square\rangle\langle\square| + |\square\rangle\langle\square|\right],\end{aligned} \tag{6}$$

with similar definitions for $\mathcal{H}_{\square}$ and $\mathcal{H}_{\square}$. Parallel dimers on the same rhombus (henceforth we refer to such configurations as *flippable rhombi*) flip with an amplitude $t$ and interact via a potential strength $v$; the sum runs over all rhombi with a given orientation. Moessner and Sondhi showed that a topologically ordered liquid phase exists over a finite region of the model's

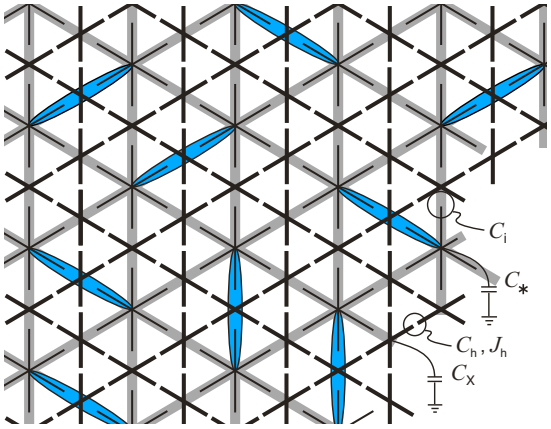


FIG. 1: (Color online) Josephson junction array used to emulate the quantum dimer model on a triangular lattice (shaded lines, ellipses represent the dimers; see Refs. [12] and [13] for details). X-shaped superconducting islands (thick black lines) form a kagome lattice with normal-state star-shaped islands (thin black lines) placed at the center of every hexagon of the kagome lattice. Cooper pairs hop between nearest-neighbor X-shaped islands with an amplitude given by the Josephson current $J_{\rm h}$. A large ratio between the capacitances $C_{\rm i}$ and $C_{\rm h}$ ensures an on-hexagon repulsion $E_{\rm hex}$ to emulate the hard-core dimer constraint. Figure adapted from Ref. [13].

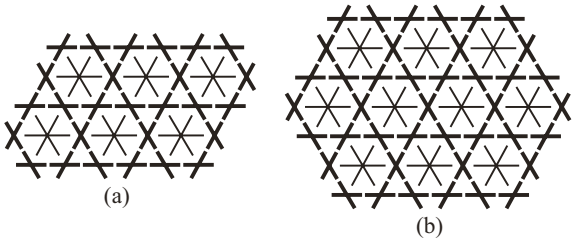


FIG. 2: Open-boundary clusters studied: (a) $N \times 2$ (here $N = 3$) hexagon ladders; (b) ten-hexagon cluster.

phase diagram ($0.82 \lesssim v/t \leq 1$), something confirmed in a number of subsequent studies [12, 17, 18, 19].

The Josephson-junction array (JJK) can be described by the generalized Bose-Hubbard model

$$\mathcal{H} = \frac{1}{2}\sum_{j,k} n_j \hat{C}^{-1}_{j,k} n_k - J_h \sum_{\langle j,k\rangle} (b_j^\dagger b_k + b_k^\dagger b_j), \qquad (7)$$

where the positions of the X-shaped islands in the array are denoted by the indices $j$ and $k$ and $\langle j,k\rangle$ represents nearest-neighbor pairs on the kagome lattice (see Fig. 1). $n_j = b_j^\dagger b_j$ is the bosonic occupation number at site $\vec{r_j}$, $J_{\rm h}$ is the Josephson current between two X-shaped islands, and $\hat{C}$ is the array's capacitance matrix. We restrict the analysis to the case of hard-core bosons [13].

### B. Two-dimer flips

In this example we focus on the off-diagonal dimer flip term $t$ in Eq. (6) from the microscopic model [Eq. (7)] with the following set of capacitances: $C_* = 1$, $C_{\rm X} = 0.25$, $C_{\rm i} = 2.5$, and $C_{\rm h} = 0.5$ (see Fig. 1). Using ENCORE these are obtained from Eq. (5): the transition amplitude between dimer configurations $|\phi_m\rangle$ and $|\phi_{m'}\rangle$ ($m \neq m'$) is the matrix element $\mathcal{H}^{\rm eff}(m,m')$. Our results have been obtained on the clusters shown in Fig. 2.

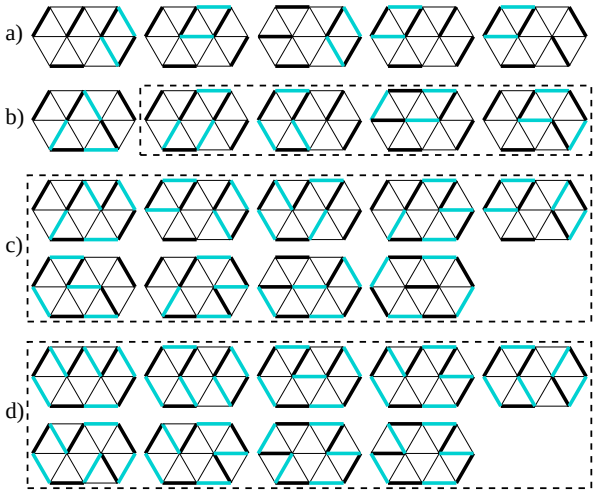


FIG. 3: (Color online) Nonequivalent dimer flips in the ten-hexagon cluster [Fig. 2(b)], comprising (a) two, (b) three, (c) four, and (d) five dimers. Dimer flips are represented by their associated *transition graph*: dimers (thick black lines) flip to new positions (thick light lines) while observing the hard-core constraint. Only the underlying triangular lattice of the JJK array is shown (shaded lines in Fig. 1). The quantity $\Sigma$ used for gauging the validity of the mapping onto a QDM is defined via the multi dimer flips enclosed by dashed lines.

The dominant off-diagonal term in the effective Hamiltonian is the two-dimer flip with amplitude $t$. This process involves the creation of a virtual state with a doubly-occupied hexagon, with energy $E_{\rm hex}$, in the kagome lattice and occurs with amplitude $t \approx J_{\rm h}^2/E_{\rm hex}$ [12, 13]. Two-dimer flips in the cluster with ten hexagons are shown in Fig. 3(a). Although the amplitudes for all these are ideally equal, there are small deviations, e.g., by the configuration of the neighboring dimers (effects of Coulomb interactions) or the open boundaries. All two-dimer flips depicted in Fig. 3(a) can be seen as being *correlated* and are considered individually at the algorithmic level.

Figure 4(a) shows results for $t$ as a function of the Josephson coupling $J_{\rm h}$ for the various clusters and in comparison to second-order perturbative results. Results for the ten-hexagon cluster are obtained by averaging the amplitudes for the processes depicted in Fig. 3(a); amplitudes for the individual processes are shown in Fig. 4(b). The results agree up to a point [vertical dashed lines in Figs. 4(a) – 4(c)] where the mapping onto a QDM fails. This agreement is an indication that, for capacitances and Josephson currents leading to a valid mapping, the low-energy physics of the JJK array is indeed described by a QDM with local dimer resonances. Furthermore, it also points to the absence of sizable finite-size effects in our results.

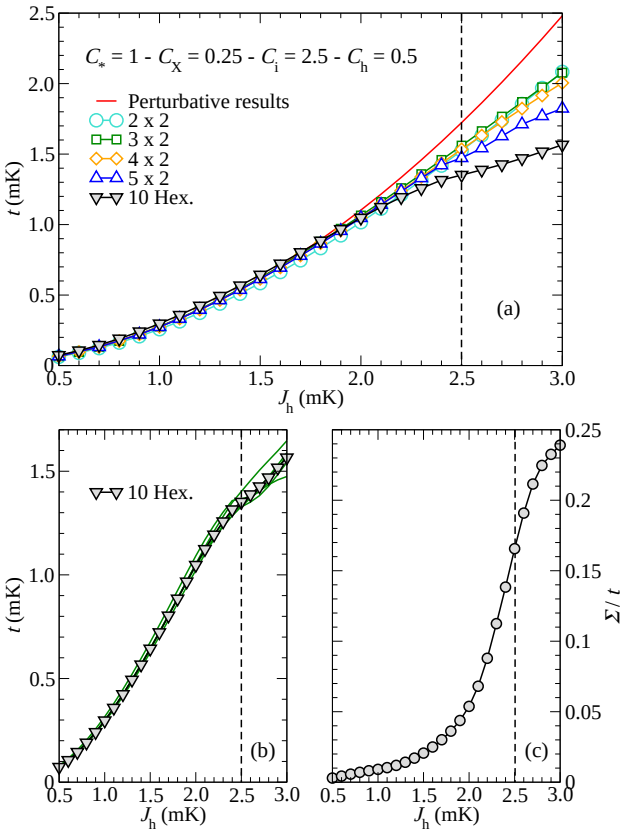


FIG. 4: (Color online) (a) Amplitude for the two-dimer flip $t$ in the JJK array obtained from the ENCORE analysis of the finite clusters shown in Fig. 2. The (red) solid curve represents second-order perturbation results. (b) Results for the ten hexagon cluster are obtained as the average (triangles) of the amplitudes of the two-dimer processes depicted in Fig. 3(a). (c) Added absolute values for the amplitudes associated to multi dimer flips ($\Sigma$). When $\Sigma$ is large the mapping onto the QDM breaks down (vertical dashed lines). Data for $C_* = 1$, $C_X = 0.25$, $C_i = 2.5$, and $C_h = 0.5$ (adapted from Ref. [13]).

### C. Multi dimer flips: Breakdown of the mapping

Whereas a standard CORE expansion proceeds by considering clusters comprising an increasing number of *sites*, an ENCORE expansion for the JJK array, due to the dimers' hard-core constraint, is performed in terms of the number of *dimers* in a cluster. The analysis of multi dimer terms can be used to gauge the validity of the mapping onto a QDM: large amplitudes for multi dimer flips indicate that the device is not properly described by the effective model. We denote the summed absolute value of the amplitudes associated to these multi dimer flips by $\Sigma$, which are directly obtained as the off-diagonal matrix elements of the effective Hamiltonian associated to the multi dimer flips enclosed by dashed lines in Figs. 3(b) – 3(d). Figure 4(c) shows $\Sigma$ as a function of the Josephson current $J_h$. A sudden increase in $\Sigma$ at the same value of $J_h$ for which different results for $t$ start to deviate from each other in Figs. 4(a) and 4(b) indicates the breakdown of the mapping. The appearance of "intruder states" in the low-energy spectrum with negligible overlap with the hard-core dimer configurations also indicate the breakdown of the mapping. The vertical dashed line in Fig. 4(c) indicates the point where the first intruder state appears. As $J_h$ increases and charge fluctuations start to dominate, intruder states displaying multiply-occupied hexagons in the JJK array violating the hard-core dimer constraint have their energy lowered, eventually causing some of the projected states $\{|\psi_m\rangle\}_1^M$ to vanish.

## IV. SUMMARY

We have presented an ENCORE algorithm suitable for constrained effective models whose basis states are not simply tensor products of local block states. We find that CORE is very effective in the design of quantum devices for emulating exotic phases. The inadequacy of the restricted set of degrees of freedom in accounting for a system's low-energy behavior is reflected by the presence of long-range terms in the effective Hamiltonian obtained from CORE and is used as a criterion in deciding on whether successful emulation is achieved.

### Acknowledgments

We thank A. Abendschein for fruitful discussions. A.F.A. acknowledges financial support from CNPq (Brazil), NIDECO (Switzerland), and ARC (Australia). H.G.K. acknowledges support from the Swiss National Science Foundation under Grant No. PP002-114713. We would like to thank the ETH Zurich Integrated Systems Laboratory and especially Aniello Esposito for computer time on the large-memory workstation "schreck."

[1] R. B. Laughlin and D. Pines, PNAS **97**, 28 (2000).
[2] C. J. Morningstar and M. Weinstein, Phys. Rev. Lett. **73**, 1873 (1994).
[3] C. J. Morningstar and M. Weinstein, Phys. Rev. D **54**, 4131 (1996).
[4] M. S. Siu and M. Weinstein, Phys. Rev. B **75**, 184403 (2007).
[5] A. Abendschein and S. Capponi, Phys. Rev. B **76**, 064413 (2007).
[6] M. S. Siu and M. Weinstein, Phys. Rev. B **77**, 155116 (2008).
[7] A. F. Albuquerque, M. Troyer, and J. Oitmaa, Phys. Rev. B **78**, 132402 (2008).
[8] J. D. Picon, A. F. Albuquerque, K. P. Schmidt, N. Laflorencie, M. Troyer, and F. Mila, Phys. Rev. B **78**, 184418 (2008).
[9] A. Abendschein and S. Capponi, Phys. Rev. Lett. **101**, 227201 (2008).
[10] D. S. Rokhsar and S. A. Kivelson, Phys. Rev. Lett. **61**, 2376

(1988).
[11] R. Moessner and S. L. Sondhi, Phys. Rev. Lett. **86**, 1881 (2001).
[12] L. B. Ioffe, M. V. Feigel'man, A. Ioselevich, D. Ivanov, M. Troyer, and G. Blatter, Nature **415**, 503 (2002).
[13] A. F. Albuquerque, H. G. Katzgraber, M. Troyer, and G. Blatter, Phys. Rev. B **78**, 014503 (2008).
[14] E. Altman and A. Auerbach, Phys. Rev. B **65**, 104508 (2002).
[15] S. Capponi, Theor. Chem. Acc. **116**, 524 (2006).
[16] Although the Lanczos [20] algorithm could in principle be used, it has problems with degenerate eigenvalues. Thus, for the smallest clusters a dense matrix eigensolver is recommended, whereas for larger clusters we use the Davidson algorithm [21].
[17] A. Ralko, M. Ferrero, F. Becca, D. Ivanov, and F. Mila, Phys. Rev. B **71**, 224109 (2005).
[18] F. Vernay, A. Ralko, F. Becca, and F. Mila, Phys. Rev. B **74**, 054402 (2006).
[19] A. Ralko, M. Ferrero, F. Becca, D. Ivanov, and F. Mila, Phys. Rev. B **74**, 134301 (2006).
[20] C. Lanczos, J. Res. Natl. Bur. Stand. **45**, 225 (1950).
[21] E. R. Davidson, J. Comput. Phys. **17**, 87 (1975).